Clay Minerals, (2018) **53**, 549–562

Ceramic properties of Uşak clay in comparison with Ukrainian clay

TURAL AGHAYEV[1,*] AND CEREN KÜÇÜKUYSAL[1]

[1] *Muğla Sıtkı Koçman University, Faculty of Engineering, Department of Geological Engineering, Kotekli, 48000, Mentese/Mugla, Turkey*

(*Received 16 November 2017; revised 16 June 2018; Accepted Manuscript published online: 27 November 2018; Version of Record published online: 12 February 2019; Guest Associate Editor: Michele Dondi*)

ABSTRACT: In this contribution, a new raw material, Uşak clay (Usc), was investigated in order to assess its potential for the ceramic industry by comparing it with a world reference ceramic material, a Ukrainian clay (Ukc). Mineralogical characterization (X-ray diffraction [XRD], scanning electron microscopy [SEM] and Fourier-transform infrared [FTIR] spectroscopy), quantitative chemical analysis (X-ray fluorescence [XRF]) and the thermal properties of Ukc and Usc samples were investigated. Additionally, Atterberg limits, particle-size distribution and cation exchange capacity of both samples were determined. Various technological properties of Ukc and Usc were determined in the temperature range 800–1430°C. The bending and compressive strengths, total linear shrinkage, colour, water absorption and unit-volume mass values were measured. The findings from these analyses show that kaolinite-dominated Ukc and quartz-dominated Usc samples differ from each other not only mineralogically, but also in terms of their chemical, physical and technological properties. The firing colour of Usc was determined as 84% white, and so this can be considered as a light firing clay. In addition, due to its low plasticity, Usc may be utilized to reduce both the plasticity of the ceramic materials and the viscosity in slip-casting applied ceramics. Furthermore, the melting temperature of 1300°C suggests that Usc cannot be classified as refractory. However, this property does suggest an economic value for Usc in terms of developing technological characteristics at lower firing temperatures.

KEYWORDS: clay mineralogy, technological properties, physicochemical properties, micromorphology, geochemistry, thermal behaviour.

From prehistoric times to the present day, clays have played an important role in agriculture, housework, construction and health, and have also been utilized in various industrial products. Because of their unique physicochemical properties, clays have been utilized as raw materials for ceramics, cosmetics, drilling muds, adsorbents, papers, cements, filtering agents, landfills, medicines, cat litter, *etc*. (Konta, 1995; Chang, 2002; Murray, 2007; Çelik, 2010; El Ouahabi, 2014; Zanelli *et al.*, 2015). The ceramic industry, which is one of the most ancient, is among the major users of clays (Smoot, 1961).

The rapid growth of the ceramic industry over the years due to greater demand than supply allowed Turkey to become Europe's third-largest and the world's sixth-largest ceramic tile exporter, according to a Turkish Ceramics Federation (TCF) report (TCF, 2009). In a more regional sense, western Turkey, especially Uşak, stands out among all other areas in this respect. However, the increasing consumption and demand for raw materials for ceramic production in Turkey clearly reveal an immediate need for the evaluation of new materials. In this context, two

This paper was originally presented during the session: 'CZ-01 – Clays for ceramics' of the International Clay Conference 2017.
*E-mail: turalaghayv@gmail.com
https://doi.org/10.1180/clm.2018.40

materials – Ukrainian clay (Ukc) and Uşak clay (Usc) – were employed together in this study to carry out an in-depth investigation of their mineralogical, chemical, physical and technological properties in order to evaluate the suitability of Usc as a raw material for production of ceramics. The Ukc, which is very famous in international ceramics markets, has been used widely because of its suitable properties (Dondi *et al.*, 2003; Zanelli *et al.*, 2015; Allegretta *et al.*, 2016); therefore, it was taken as a reference material in the present study to assess the suitability of Usc for ceramics.

MATERIALS AND METHODS

Ukrainian and Uşak clays , which are used widely for ceramics production were studied. Numerous 10-kg bags of Ukc and Usc samples were collected from piles in a ceramics factory in Uşak, Turkey. In order to achieve greater homogeneity in the samples, the sampling procedure included extraction from a number of parts of each pile and the samples were mixed thoroughly to achieve a composite sample. Approximately 90-kg samples for technological tests and 5-kg samples for mineralogical, geochemical and physical-characterization tests were prepared.

Mineralogical and chemical analysis

The mineralogical composition of the samples studied was determined by XRD analysis, using a Panalytical Expert Pro diffractometer equipped with a Cu tube at a 40-kV voltage and a 30-mA current at the Mineralogy–Petrography Laboratory, General Directorate of Mineral Research and Exploration, Turkey. The XRD traces were obtained in the range 4–70°2θ with a scanning rate of 2°/min. Mineral identification was based on the combined methods of Thorez (1976), Chen (1977) and Moore & Reynolds (1989). Semi-quantitative mineralogical analysis of both samples was performed using the method based on chemical analysis by XRF.

The clay mineralogy was determined from the clay (<2 μm) fractions which were separated from the bulk samples at the Clay Mineralogy Laboratory of the Engineering Faculty, Mugla Sitki Kocman University, Turkey. The clay-size fractions were analysed by XRD (GNR APD 2000 PRO diffractometer) using a Cu tube operated at a tube voltage of 40 kV and a current of 30 mA over the range 2–30°2θ at a scanning rate of 2°/min, applying air-drying (AD), ethylene glycol (EG) solvation and heating to 500°C in the X-ray Diffraction Laboratory of the Geological Engineering Department at Pamukkale University. EG solvation was used to detect swelling in the clays, whereas heat treatment at 500°C was used to identify the presence of kaolinite.

Whole-rock chemical analysis of the major elements was performed by Thermo ARL XRF on powder pellets at the Analytical Chemistry Laboratory of the General Directorate of Mineral Research and Exploration.

The Ukc and Usc clay samples were also examined by SEM (JEOL JSM-7600F) at an accelerating voltage of 15 kV to identify the micromorphology of the minerals at the Research and Application Centre for Research Laboratories of Mugla Sitki Kocman University. Elemental characterization of the minerals present was performed with energy-dispersive X-ray spectrometry (EDS; Oxford Instruments).

Fourier Transform Infrared (FTIR) spectra were collected at the Mineralogy–Petrography Laboratory of the General Directorate of Mineral Research and Exploration, using a Perkin Elmer Spectrum (version 10.03.07) spectrophotometer. Spectra were recorded in transmission mode over the range 450–4000 cm^{-1}, with a resolution of 4 cm^{-1} and 10 scan signal averages for each sample.

The cation exchange capacity (CEC) of the samples was measured at the Clay Mineralogy Laboratory of the Engineering Faculty, Mugla Sitki Kocman University, by methylene blue adsorption. Each 50-g clay sample was passed through a no. 200 mesh (equivalent to a 0.074 mm opening sieve) and mixed with 50 mL of distilled water. Methylene blue solution was prepared according to the method of Jones (1964).

Thermal analysis

The thermal behaviour of the Ukc and Usc samples was studied using a Rigaku Thermoflex TG 8110 instrument over the range 25–1050°C at a rate of 10°C/min at the Industrial Raw Materials and Ceramic Materials Research Laboratory of the General Directorate of Mineral Research and Exploration.

Physical properties

The liquid limit (LL), plastic limit (PL) and particle-size distribution of the samples were determined at the Clay Mineralogy Laboratory of the Engineering Faculty, Mugla Sitki Kocman University, using a Casagrande apparatus according to Bowles (1992). 250 g of each sample was passed through a no. 40 mesh (equivalent to a 0.0165 mm sieve). The plasticity

https://doi.org/10.1180/clm.2018.40 Published online by Cambridge University Press

index (PI) was calculated by the difference between the LL and PL.

For the particle-size distribution, the coarse fraction from each sample was separated by wet sieving based on TS 4790 (1986) standards. Silt-size (<63 μm) and clay-size (<4 μm) fractions were measured by hydrometer analysis using a 152 H hydrometer according to Bowles (1992). To avoid flocculation, 5 g of sodium hexametaphosphate ($NaPO_3$) was added to each sample.

Technological tests

The technological tests on the Ukc and Usc samples were performed at the Industrial Raw Materials and Ceramic Materials Research Laboratory of the General Directorate of Mineral Research and Exploration. Size fractions of <2.8 mm from each sample were prepared to form rectangular prism bodies prism bodies 25 mm × 25 mm × 115 mm in dimension for technological tests. The bodies were dried overnight at room temperature and then were dried again in a furnace first for 4 h at 55°C and then for 24 h at 110°C to determine the linear drying shrinkage and dry-bending strength. To measure the total linear shrinkage, bending strength and compressive strength at various temperatures, each body from the Ukc and Usc samples was fired in a kiln at 800°C, 900°C, 1000°C, 1100°C, 1150°C, 1300°C and 1430°C with a heating rate of 150°C/h. Linear drying and total linear shrinkage values were calculated using equation 1:

$$\%S_d = L_p - L_d/L_p \times 100 \quad (1)$$

where S_d is the % linear drying shrinkage or total linear shrinkage L_p is the length before drying or firing temperatures and L_d is the length after drying or firing temperatures.

The bending-strength test was performed at 4.5 N/min load on the dried and fired bodies. The bending strength values were calculated using equation 2:

$$M = 3(P \times L)/2(a \times h)^2 \quad (2)$$

where M is the dry or fired bending strength (N/mm^2), P is the breaking (bending) force (N), L is the distance between supports (mm), a is the width of the breaking point of the body (mm) and h is the thickness of the breaking point of the body (mm) (TS 4790, 1986).

For the compressive strength tests, two new bodies from each sample with 10–15 cm^2 surface area and 1.5 cm height were formed by cutting them from the previously fired bodies. The compressive strength test was carried out by applying the stress at the same time to both sides of each body with an increasing pressure rate of 4.9–5.9 bar for every second until body failure. Compressive strength values were calculated using equation 3:

$$F_b = P_k/A_0 = k \quad (3)$$

where F_b is the compressive strength of the body (bar), P_k refers to the load applied to break the body (N), A_0 stands for the surface area of the body (cm^2) and k is the shape factor of the body (standard of 0.5) (TS 4790, 1986).

Colour changes were identified using a Minolta Chroma Meter CR-300 model reflected light colorimeter after firing of the bodies at 800°C, 900°C, 1000°C, 1100°C, 1150°C, 1300°C and 1430°C.

Water adsorption was determined tested after firing the bodies at 800°C, 900°C, 1000°C and 1100°C separately by keeping them in water for 24 h and after boiling them in water for 5 h using TS EN 772-21 (2011) and TS EN 772-7 (2000), respectively.

The unit volume mass property of each body was calculated at 800°C, 900°C, 1000°C and 1100°C using TS EN 771-1 (2012). In addition, the firing status was recorded by naked-eye observation and the hardness of the bodies fired at the aforementioned temperatures was recorded according to the Mohs hardness scale. The percentages of $CaCO_3$ were determined according to TS 4790 (1986) using equation 4:

$$\%CaCO_3 = 0.1604 \times (P.V)/(T.a) \quad (4)$$

where P is atmospheric pressure (mmHg), V is volume of emitted CO_2 gas (mL), T is room temperature in K (T°C + 273) and a is the amount of sample (g).

RESULTS

Mineralogical and chemical characterization

The results of XRD analysis of the bulk Ukc and Usc samples are given in Fig. 1a and 1b, respectively. The bulk compositions of both samples have the same mineral assemblages in terms of total clay (including kaolinite and illite), quartz and dolomite (Fig. 1a and 1b). Total clay was identified from the reflections at 4.44–4.48 Å at ~19°2θ. Quartz was identified from the reflection of 3.35 Å at 26.5°2θ and dolomite from the major peak at 2.89–2.90 Å at 31°2θ (Fig. 1b).

The clay fractions of Ukc and Usc show very intense reflections of kaolinite at 7 and 3.58 Å (Fig. 2a,b) in AD XRD patterns. Kaolinite did not react with EG, but collapsed after heating at 500°C (Fig. 2a,b). Illite was

https://doi.org/10.1180/clm.2018.40 Published online by Cambridge University Press

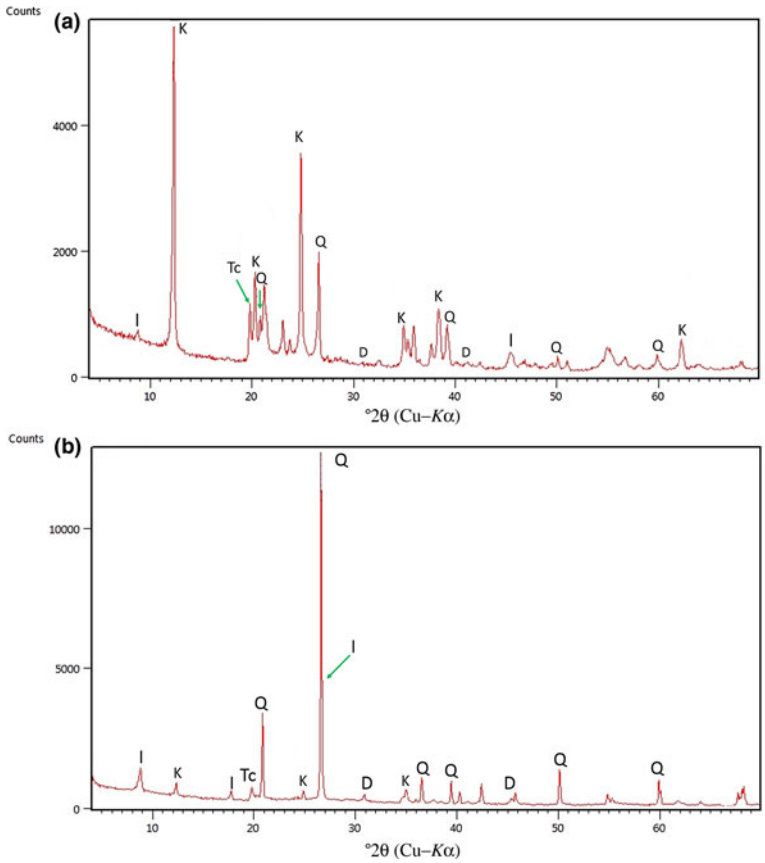

FIG. 1. XRD traces of randomly oriented powders of (a) Ukc and (b) Usc. Q = quartz; D = dolomite; I = illite; K = kaolinite; Tc = total clay.

identified from the 10 Å peak at 8.2°2θ (Fig. 2a,b) in AD conditions; which was not affected by EG solvation and heating to 500°C (Figs 2a,b).

Based on the chemical analysis, the bulk mineralogical composition of the Ukc sample is characterized by the dominance of kaolinite (51%), quartz (35%) and small amounts of illite (8%) and dolomite (6%) (Table 1). The Usc sample, on the other hand, has more abundant quartz (56%) and relatively large amounts of illite (26%) in association with small amounts of kaolinite (12%) and dolomite (6%) (Table 1).

The results of bulk geochemical analysis by XRF are given in Table 1. Both Ukc and Usc samples are characterized by high SiO_2 and relatively low Al_2O_3 contents. The amount of alkals (K_2O and Na_2O) is small (1%) in the Ukc sample, represented by the small amount of illite, while it is relatively high (3%) in the Usc sample, confirming the greater amount of illite in the compositions. For both samples, very small amounts of CaO and MgO (2.0% for Ukc and 2.2% for Usc) indicate very small amounts of dolomite in their compositions. In addition, Fe_2O_3, which plays an important role in colouring the red fired products, is present in very small amounts for the Ukc sample (0.3%) and the Usc sample (1.2%). Other oxides (*e.g.* CaO, MgO, MnO and TiO_2) also contribute to this property (Kreimeyer, 1987) and the degree of firing, together with Al_2O_3. The relatively high value of loss on ignition (LOI) in the Ukc sample (8.37%) with respect to that in the Usc sample (4.27%) is associated with the larger amount of kaolinite.

Large $CaCO_3$ contents may cause cracks on the fired bodies, calcification in kilns and high porosity and water absorption values, all of which affect directly the quality of the ceramic raw materials (TS 4790, 1986).

https://doi.org/10.1180/clm.2018.40 Published online by Cambridge University Press

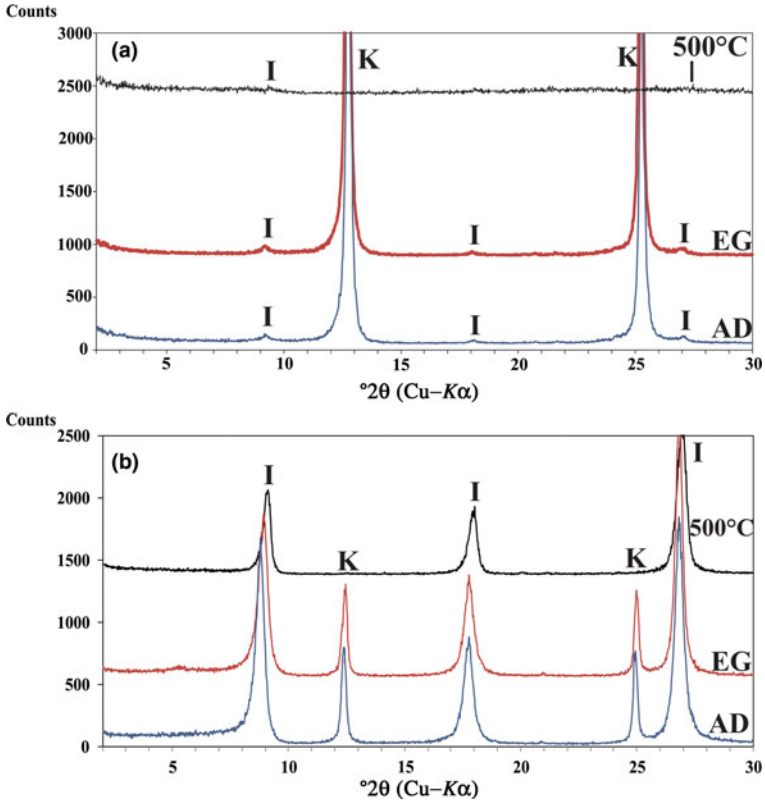

FIG. 2. XRD patterns of: (a) oriented Ukc samples and (b) oriented Usc samples air-dried (AD), ethylene glycol solvated (EG) and heated at 500°C. I = illite; K = kaolinite.

TABLE 1. Bulk chemical and mineralogical compositions (mass %) of the Ukc and Usc samples.

Component	Ukc	Usc
SiO_2	63.4	73.2
TiO_2	0.5	0.1
Al_2O_3	24.0	15.0
Fe_2O_3 total	0.3	1.2
MgO	0.2	0.8
CaO	1.8	1.4
Na_2O	0.1	0.1
K_2O	0.9	3.1
LOI	8.37	4.27
Quartz	35	56
Dolomite	6	6
Kaolinite	51	12
Illite	8	26
Total	100	100

The $CaCO_3$ contents was 2.0% in the Usc sample and 2.92% in the Ukc sample. The micromorphology of the minerals observed by field-emission gun–scanning electron microscopy (FEG-SEM) is characterized by stacked platelets ('booklets') of kaolinites in the Ukc sample (Fig. 3a,b) with almost equal intensities for Al and Si EDS spectra (Fig. 3c,d). The SEM images of the Usc sample show quartz crystals with conchoidal fracture partly coated with kaolinite platelets (Fig. 3e), which is represented by an intense Si peak in the EDS spectrum (Fig. 3g). Additionally, the mosaic form of kaolinite together with filamentous illite were observed in the Usc sample (Fig. 3f), as was shown in the EDS results for both morphologies (Fig. 3h).

The results of the thermal analysis of the Ukc and Usc samples are shown in Figs 4a and 4b, respectively. The weak endothermic peak near 100° C for the Usc sample is related to the removal of adsorbed water, which was confirmed by the first

https://doi.org/10.1180/clm.2018.40 Published online by Cambridge University Press

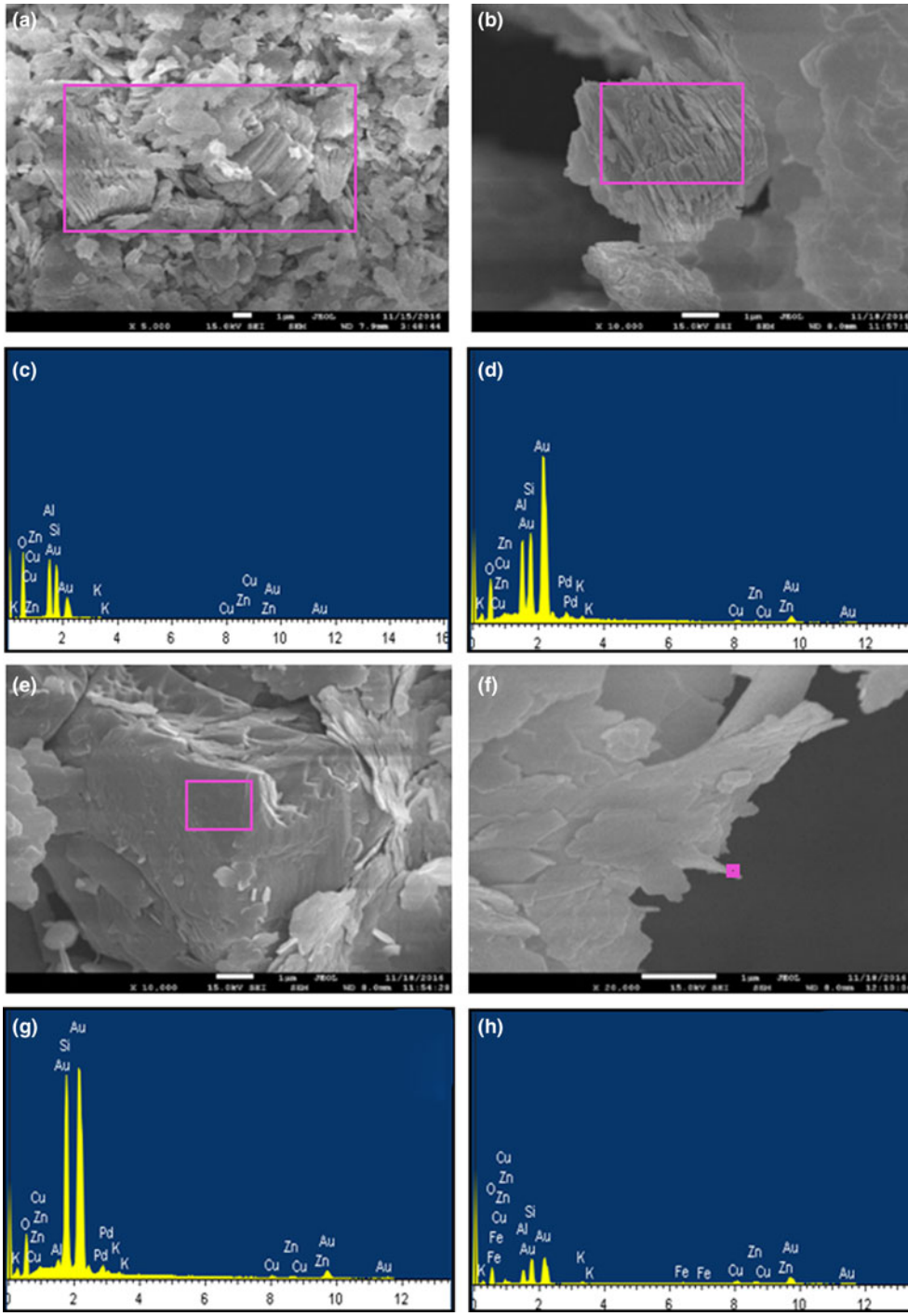

FIG. 3. SEM images and EDS of the Ukc and Usc samples: (a, b) kaolinite booklets in the Ukc sample; (c, d) EDS spectra of (a) and (b); (e) quartz crystals with conchoidal fracture partly coated with kaolinite platelets; (g) EDS spectrum of (e); (f) mosaic form of kaolinite together with filamentous illite in the Usc sample; (h) EDS spectrum of (f).

https://doi.org/10.1180/clm.2018.40 Published online by Cambridge University Press

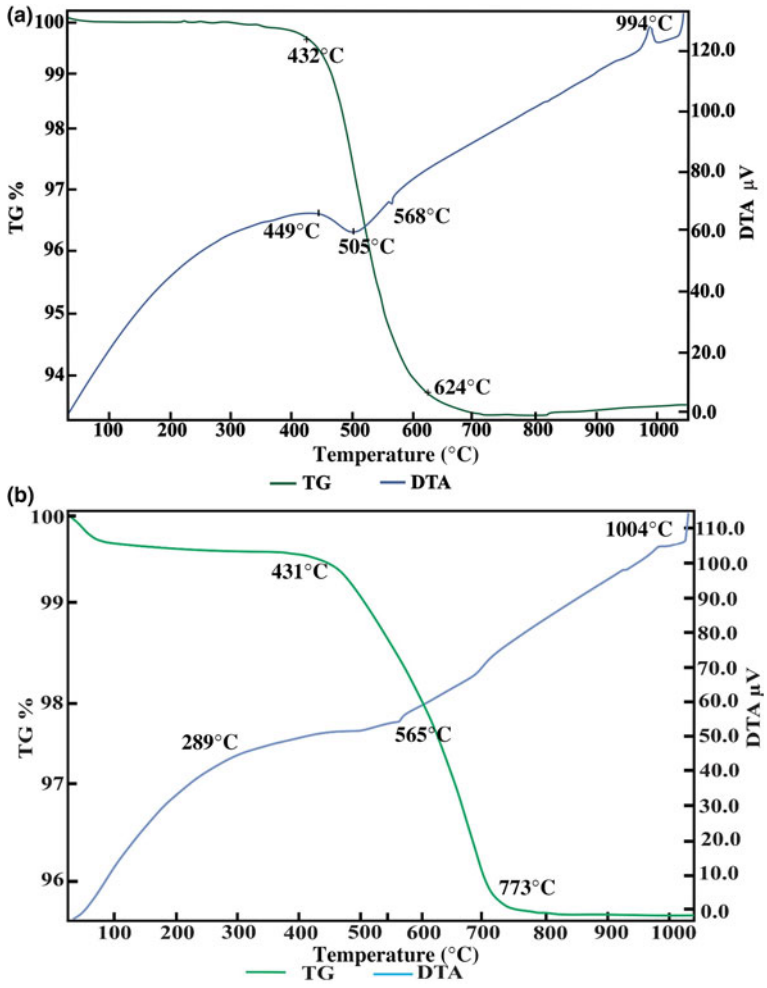

FIG. 4. DTA/TG curves of (a) Ukc and (b) Usc.

mass loss on thermogravimetry (TG) (Fig. 4b). Due to the dehydroxylation of kaolinite and illite, broad endothermic peaks at 505°C and 495°C were observed on differential thermal analysis (DTA) diagrams of Ukc (Fig. 4a) and Usc (Fig. 4b), respectively. These events cause the transformation of kaolinite to metakaolinite (Brindley & Nakahira, 1959). A relatively sharp peak at 568°C for Ukc (Fig. 4a) and a relatively weak one at 565°C for Usc (Fig. 4b) were attributed to the α–β quartz transformation (Grim & Rowland, 2009). The weak exothermic peak at 1004°C for Usc (Fig. 4b) and a slightly more intense one at 994°C for Ukc (Fig. 4a) are attributed to the formation of mullite (Insley & Ewell, 1935; Brindley & Nakahira, 1959; Çelik, 2010). Second exothermic peaks were also recorded at >1050°C for the Ukc sample (Fig. 4a) and at 1040°C for the Usc sample (Fig. 4b). The mass losses were ∼6.7% for Ukc (Fig. 4a) and 4.5% for Usc (Fig. 4b).

The ternary diagram of SiO_2–Al_2O_3–other major oxides of Fabbri & Fiori (1985) was used to compare the samples chemically with other commercial clay raw materials for ceramics (Fig. 5). On this diagram, the Ukc sample is projected in the same region as the clays of German and English white stoneware, while the Usc sample plots very close to the region for white stoneware from Germany (Fig. 5).

https://doi.org/10.1180/clm.2018.40 Published online by Cambridge University Press

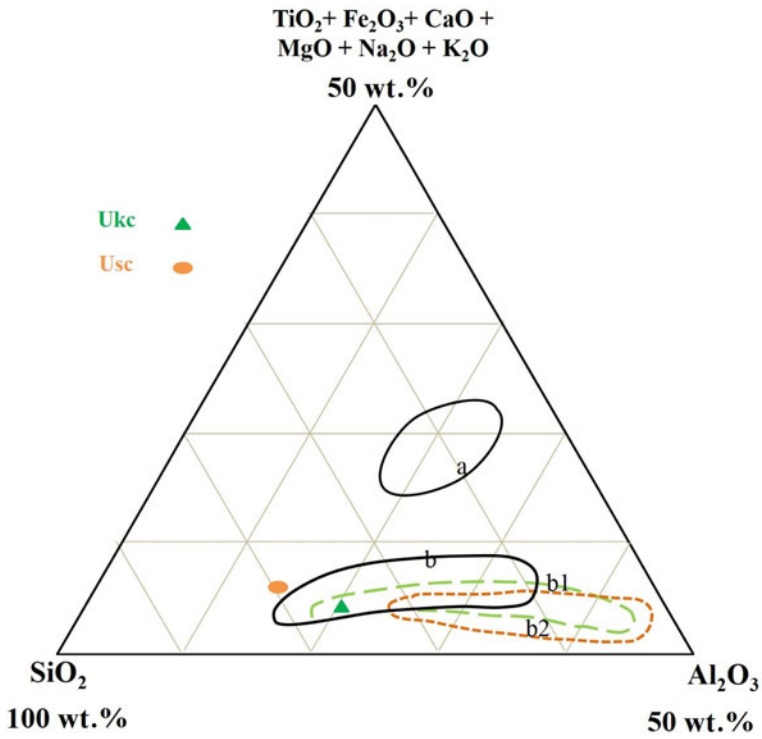

FIG. 5. SiO_2–Al_2O_3–other oxides ternary diagram of Ukc and Usc: a = red stoneware (Italy); b, b1, b2 = white stoneware (German, English, and French, ceramics industries, respectively). Data from Fabbri & Fiori (1985).

The infrared spectra for the bulk samples are shown in Figs 6a and 6b. The presence of clay minerals in samples of both Ukc and Usc was confirmed by the absorption bands at 3700–3620 cm^{-1} (Azzi *et al.*, 2016). The sharp OH-stretching band at 3695–3670–3652 and 3620 cm^{-1} coupled with OH-deformation bands of 938 and 913 cm^{-1} are characteristic of kaolinite in the Ukc sample (Udvardi *et al.*, 2014; Bennour *et al.*, 2015a; Zaied *et al.*, 2015) (Fig. 6a). The relatively broad absorption band at 697 cm^{-1} in the Si–O bending region is attributed to quartz in the Ukc sample (Fig. 6a). A weak band near 1030 cm^{-1} in the Si–O stretching region together with a 3620 cm^{-1} band in the OH-stretching region confirm the presence of illite also (Udvardi *et al.*, 2014; Bennour *et al.*, 2015b; Zaied *et al.*, 2015) (Fig. 6a). Strong absorption bands of quartz at 692 and 796 cm^{-1} were recognized in the Si–O bending and Si–O stretching regions of the infrared spectra of the Usc sample, respectively (Udvardi *et al.*, 2014; Bennour *et al.*, 2015b) (Fig. 6b). Intense bands at 3620–3651–3695 cm^{-1} together with a 913 cm^{-1} OH deformation band demonstrate the presence of kaolinite in the Usc sample (Udvardi *et al.*, 2014; Azzi *et al.*, 2016) (Fig. 6b). The diagnostic band of dolomite in the Usc sample at 1431 cm^{-1} is attributed to CO_3 stretching (Udvardi *et al.*, 2014; Bennour *et al.*, 2015b) (Fig. 6b).

The CEC values for both clay materials determined by the methylene blue test (Jackson, 1979) were 3.73 meq/100 g for the Ukc sample and 5.97 meq/100 g for the Usc sample. In both samples, the CEC values are typical of clays with small specific surface areas (Bain *et al.*, 1994). As the percentages of the finer fractions of the Ukc samples are much greater than those of the Usc samples and the specific surface area of kaolinite is smaller than that of illite, these findings are in agreement with the mineralogical results.

Physical properties

The PL, LL and PI values of the Ukc and Usc samples are given in Table 2. The LL values of Ukc and Usc were 38.0% and 25.7%, respectively, while the PL values were 23.8% and 14.9%, respectively. Based on

https://doi.org/10.1180/clm.2018.40 Published online by Cambridge University Press

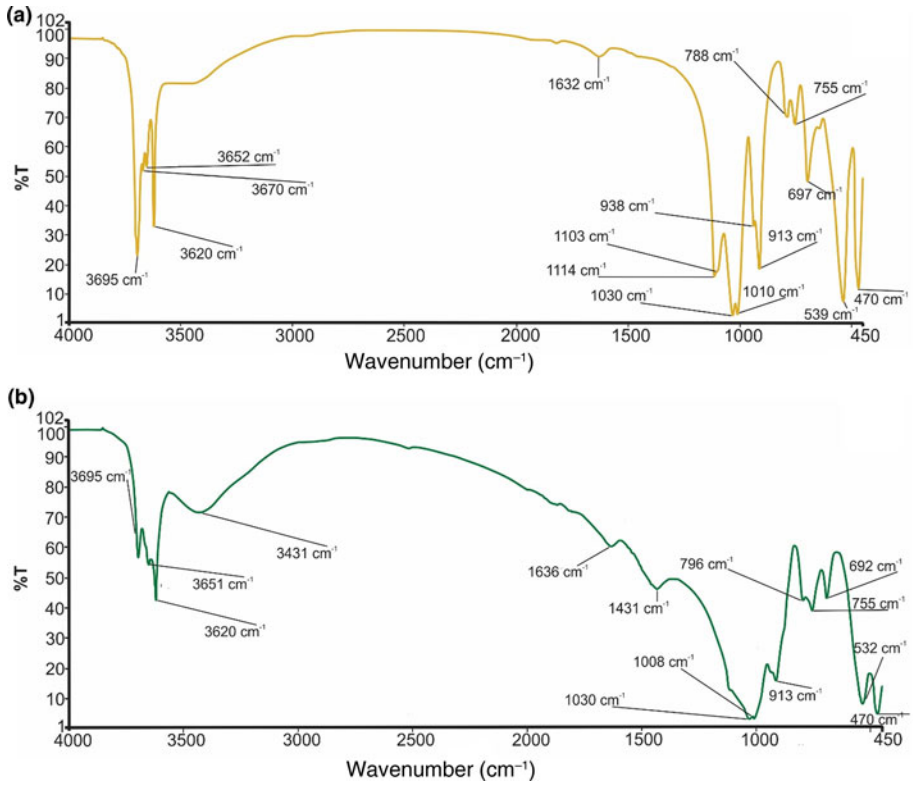

FIG. 6. FTIR spectra of (a) Ukc and (b) Usc.

the Atterberg limits, the PI is calculated as 14.2% for Ukc and 10.8% for Usc.

According to the calculated consistency limits plotted on the Holtz & Kovacs (1981) diagram (Fig. 7), the Ukc sample resides in the medium plastic zone while the Usc sample is located in the low plastic region. The presence of quartz and the absence of interstratified I-S and expandable clays tend to reduce the LL, PI and CEC values, which is also relevant in the present study (Bennour *et al.*, 2015).

According to Çelik (2010), the high-plastic raw materials may cause hard drying and reducing the wearing down of the equipment for grinding and conformation (Monteiro & Vieira, 2004).

The particle-size distributions of the raw materials are important for many studies, and a fine fraction size distribution is diagnostic of ceramic products (Mahmoudi *et al.*, 2008; Çelik, 2010). The clay fraction content (<4 μm) was ~54% for the Ukc sample, and 25% for the Usc sample (Table 2). The silt fraction contents (4–63 μm) were ~32% for the Ukc sample and 58% for the Usc sample. The sand fraction content (>63 μm) was ~14% for the Ukc sample and ~18% for the Usc sample (Table 2).

TABLE 2. Dry-bending strengths, linear shrinkage, Atterberg limits, CEC values and particle-size distributions of Ukc and Usc.

Parameter	Unit	Ukc	Usc
Technological properties			
Dry-bending strength	MPa	0.29	0.68
Linear drying shrinkage	Mass %	3.36	4.11
Consistency limits			
LL	Mass %	38.0	25.7
PL	Mass %	23.8	14.9
PI	Mass %	14.2	10.8
CEC	meq/100 g	3.73	5.97
Particle-size distribution			
Sand (>63 μm)	Mass %	14	18
Silt (4–63 μm)	Mass %	32	58
Clay (<4 μm)	Mass %	54	25

https://doi.org/10.1180/clm.2018.40 Published online by Cambridge University Press

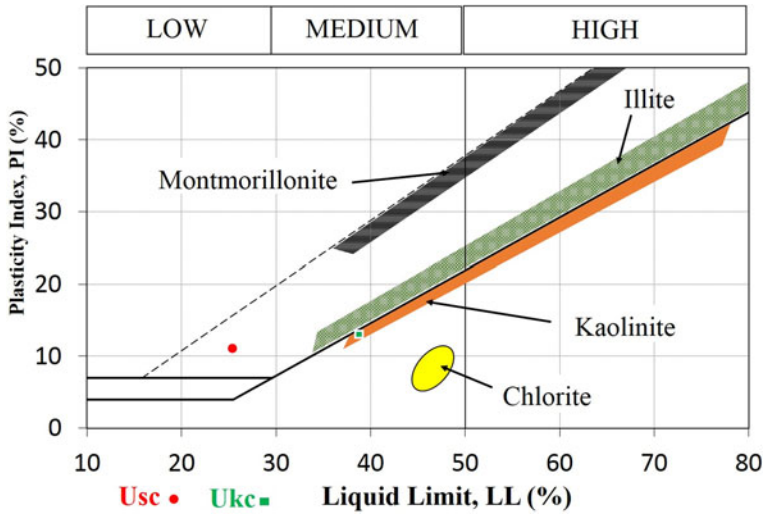

FIG. 7. LL and PI values of the Ukc and Usc samples on the Holtz & Kovacs (1981) diagram.

Technological properties

The technological properties of the samples studied are listed in Table 3. Ukc reached its maximum lightness (L*) value (94.21%) at 1100°C. In contrast, the maximum L* value for Usc was observed at 1000°C (83.59%). The hardness values measured for both samples were almost identical over the whole temperature range. However, the compressive strength of Usc was greater at all tested temperatures (except at 800°C) than that of Ukc. The compressive strength of Usc reached 13 MPa at 1300°C, while Ukc showed a compressive strength of 9.5 MPa. The compressive strength of Ukc decreased at 1430°C.

The firing characteristics of the unit volume mass of the bodies prepared from the samples studied were demonstrated with respect to temperature (Fig. 8a). There were no major changes in the measured unit volume mass for either Ukc or Usc. For Ukc, a very slight increase was observed between 800°C and 900°C and then a constant value was obtained between 900°C and 1100°C. The unit volume mass for Usc was slightly higher than for Ukc, increasing slightly between 1000°C and 1100°C because of the substantial glassy phase, the presence of which was confirmed by the exothermic peak of the Usc sample at 1004°C (Fig. 4b).

Water absorption is a technological parameter that permits the classification of ceramic tiles (Çelik, 2010). The water absorption values for Ukc are much greater than those for Usc (Fig. 8b). Ukc (24 h) and Usc (24 h) indicate that the bodies were kept underwater for 24 h. The boiling procedure for Ukc (5 h) and Usc (5 h) was carried out to measure the absorption values at 5 h as well. Generally, water absorption of the bodies is influenced by the boiling process. Sample Usc (5 h) displayed greater water absorption values (15.24–17.70%) with increasing temperature (800–1100°C) (Fig. 8b). The water absorption of Ukc (5 h) was virtually constant over the same temperature range (26.35–25.73%) (Fig. 8b).

The total linear shrinkage of Usc and Ukc was plotted on a total linear shrinkage (%) *vs.* temperature diagram (Fig. 9). The linear shrinkage values of Usc are mostly greater than those of Ukc between 800°C and 1430°C. For Usc, the total linear shrinkage values increased greatly over 1000°C with a major change (11.89%) observed at 1300°C (Fig. 9). For Ukc the greater total linear shrinkage values (3.86–6.64%) were observed above 1100°C. Because the Usc sample had melted completely at 1430°C, the total linear shrinkage values were not recorded at high temperatures.

The bending strengths of the Ukc and Usc in the temperature range of 800–1430°C, are shown in Fig. 10. Temperature clearly affects the bending strength of both samples. Usc reached a maximum bending strength rate of 19.4% at 1300°C, while the bending strength of Ukc was 2.23% at the same temperature.

The Ukc and Usc were projected in the ternary diagram of Dondi *et al.* (2014) (Fig. 11) for

https://doi.org/10.1180/clm.2018.40 Published online by Cambridge University Press

TABLE 3. Technological properties of Ukc and Usc.

Temperature (°C)			800	900	1000	1100	1150	1300	1430
Usc	Firing colour/status		Beige/sintered	Beige/sintered	Beige/sintered	Beige/sintered	Sintered	Melting starts	Bodies melted completely
	Colour properties	L*	81.35	82.59	83.59	82.34	80.18	73.39	
		a*	+5.13	+4.87	+4.47	+2.97	+3.53	−0.54	
		b*	+13.02	+12.58	+12.76	+15.68	+5.37	+9.16	
	Compressive strength	MPa	4.0	5.3	5.4	7.1	8.2	13.0	
	Hardness	Mohs	2	2	2	3	–	–	–
Ukc	Firing colour/status		Beige/sintered	Beige/sintered	Beige/sintered	Beige/sintered	Beige/sintered	Beige/sintered	Beige/sintered
	Colour properties	L*	92.32	93.26	93.76	94.21	94.16	89.19	89.14
		a*	+0.29	−0.24	−0.04	−0.12	+0.36	+0.45	−0.81
		b*	+4.17	+3.50	+2.43	+2.02	−3.8	+7.75	+5.83
	Compressive strength	MPa	4.2	4.7	5.1	5.6	6.0	9.5	8.0
	Hardness	Mohs	2	2	2	3	–	–	–

L* = value of white colour; a* = redness when positive and greenness when negative; b* = yellowness when positive and blueness when negative.

classifcation of light-firing clays. Ukc is plotted in an area dominated by low-grade kaolin clays, while Usc is plotted within an area dominated by raw kaolin and kaolinitic loam.

DISCUSSION

The mineralogical, physico-chemical and technological characteristics of Usc clay from Turkey were investigated and compared with a reference clay, Ukc. The smaller amount of Fe_2O_3 and larger amount of Al_2O_3 yielded a white colour for Ukc (Dondi *et al.*, 2014). In the ternary diagram of Fabbri & Fiori (1985) (Fig. 5), Ukc is projected in the region for German and English white stoneware, whereas. The Usc sample plots close white stoneware used in the German industry. This is due to the small Fe_2O_3 contents of both samples as the amount of Fe_2O_3 (<3%) allows the classification of Ukc and Usc samples as light-firing clays (Dondi *et al.*, 2014). Besides affecting the colour, Fe_2O_3 acts as flux with MgO, K_2O and Na_2O (Dondi *et al.*, 1999; Çelik, 2010; Mefire *et al.*, 2016). The total amount of fluxing oxides in Usc (Table 1) provides a better explanation of its low melting temperature (1300°C; Table 3). The small amount of fluxing oxides in Ukc is associated with the kaolinite content (Monteiro & Vieira, 2004). Moreover, the large Al_2O_3 content is related to the presence of kaolinite and illite in the mineralogical compositions of both samples (Murray, 2007). On the other hand, Usc showed better technological characteristics when fired, which is also due to the presence of fluxing oxides in Usc. The decrease in water absorption and increase in total linear shrinkage, bulk density, bending strength and compressive strength observed at temperatures >1000°C are probably related to the formation of new phases, as observed in the DTA curve for Usc (Fig. 4b) at 1004°C and 1040°C. Sharp increase in the bending strength, total linear shrinkage and compressive strength of Usc were also recorded at 1300°C, which was the starting temperature of melting (Table 3). The bulk density value of Ukc (1.47 g/cm^3) at 1100°C is less than that of Usc (1.66 g/cm^3). The mechanical strength of the ceramic raw materials increased with bulk density (Lee & Yeh, 2008; Ngun *et al.*, 2011). Due to the sharp increase in bending strength at 1300°C (Fig. 10), it is expected that the bulk density would increase at the same temperature. The water absorption of Ukc is greater than that of Usc at all temperatures. The water-absorption value of Ukc might be related directly to the high porosity of the fired body,

https://doi.org/10.1180/clm.2018.40 Published online by Cambridge University Press

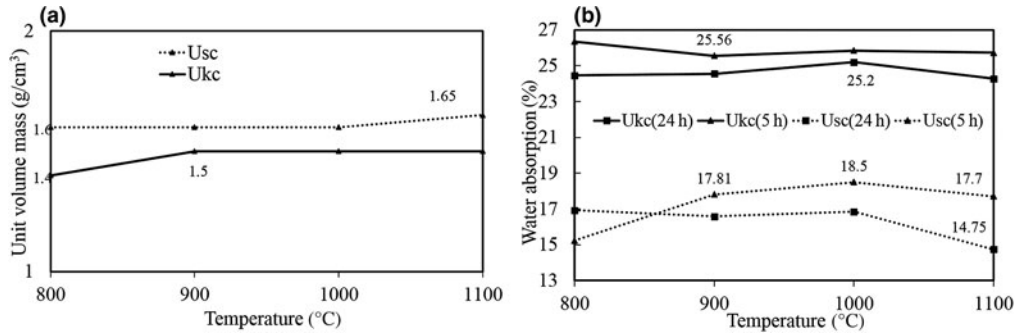

FIG. 8. (a) Unit-volume mass and (b) water-absorption values of fired Ukc and Usc samples at various temperatures.

which induces a low mechanical strength in Ukc (Dondi *et al.*, 2001) (Fig. 8b). The water absorption for bricks should be <25%, whereas in roof tiles it should be >20% (Milheiro *et al.*, 2005). Furthermore, in the study by Cengiz & Kuşçu (2010), the water absorption was 8–18%, dry and firing shrinkage values were ≤10% at 1100°C and plasticity index water was 25–35% at 1000°C. Therefore, Usc might be considered to be suitable for bricks and tiles. The Mohs hardness values of both Ukc and Usc were 2 at between 800°C and 1000°C, increasing to 3 at 1100°C. In Fig. 11, Usc was classified as raw kaolin and kaolinitic loam clay (Dondi *et al.*, 2014), suggesting that it might be used as a raw material for ceramics due to the abundance of quartz, kaolinite and flux materials. This type of clay material might also be suitable as a raw material for tile manufacture, subject to economics. In addition, Usc may also be considered as a versatile raw material suitable for use in vitrified bodies in amounts of up to 20–25% (Dondi *et al.*, 2014). The Usc sample, due to its melting at 1430°C, is not classified as refractory; however, the kaolinite-rich Ukc sample, with its melting point at ~1850°C, clearly has refractory properties (Murray, 2007).

CONCLUSION

The ceramic properties of Usc clay from Turkey were compared with those of a reference clay from the Ukraine. Mineralogical, chemical, physical and technological analyses were performed on both samples, and the findings compared. The small amount of Fe_2O_3 content and the abundance of Al_2O_3 in Usc and Ukc led to a white colour after firing. The abundance of fluxing oxides and the smaller amounts of fire-resistant refractory minerals caused melting of Usc at 1300°C. The formation of new phases at 1004°C and 1040°C explain the remarkable improvements in of the technological properties of Usc at temperatures of >1000°C. The small amount of fine-grained material in Usc suggests that additional grinding of the coarser fraction might be necessary prior to use.

Because of the poor plasticity and large amount of SiO_2 in Usc, it can be used to reduce the plasticity and

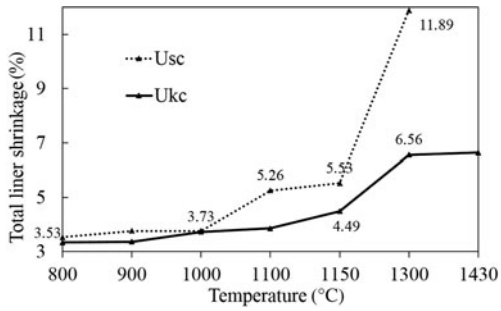

FIG. 9. Total linear shrinkages of the fired Ukc and Usc samples at various temperatures.

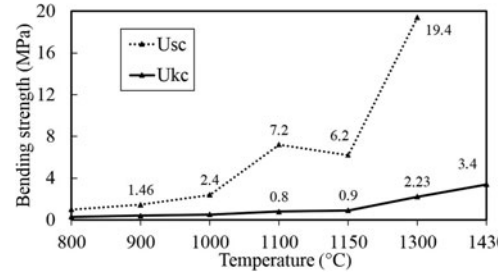

FIG. 10. Bending-strength values of Ukc and Usc at various temperatures.

https://doi.org/10.1180/clm.2018.40 Published online by Cambridge University Press

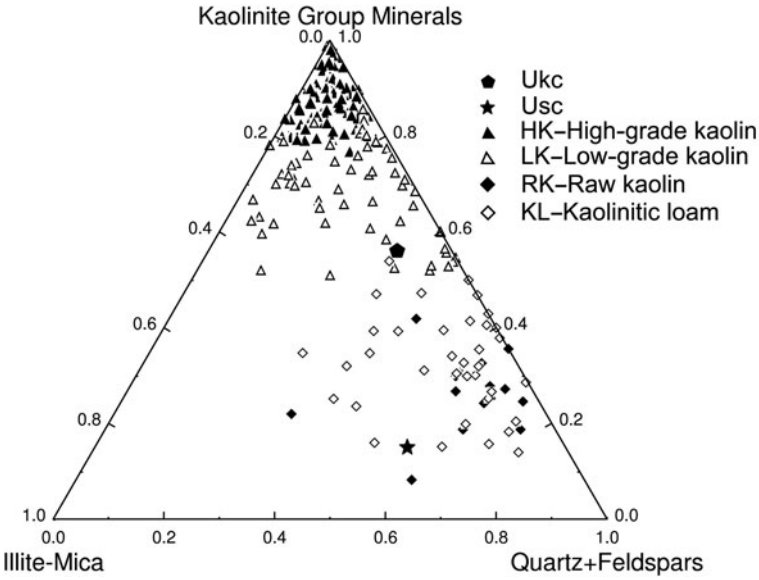

FIG. 11. Projection of Ukc and Usc in the mineralogical composition chart of light-firing clays for ceramic tiles (Dondi *et al.*, 2014).

viscosity of the slip-casting applied ceramics. On the other hand, the white firing colour of Usc rendered it suitable for use in light-coloured ceramics. Because the melting of Usc started at 1300°C, it is not classified as refractory. However, the low melting point renders Usc economically viable for development of technological characteristics at lower firing temperatures.

ACKNOWLEDGEMENTS

The authors thank Muğla Sıtkı Koçman University for financial support under Project 15/195. The authors are also grateful to Michele Dondi (ISTEC CNR) and Prof. Dr Ömer Bozkaya (Pamukkale University) for their constructive comments. The reviewers of this contribution are acknowledged for their invaluable comments which improved the quality of the manuscript significantly.

REFERENCES

Allegretta I., Pinto D. & Eramo G. (2016) Effects of grain size on the reactivity of limestone temper in a kaolinitic clay. *Applied Clay Science*, **126**, 223–234.

Azzi A.A., Osacký M., Uhlík P., Čaplovičová M., Zanardo A. & Madejová J. (2016) Characterization of clays from the Corumbataí formation used as raw material for ceramic industry in the Santa Gertrudes district, São Paulo, Brazil. *Applied Clay Science*, **132–133**, 232–242.

Bain D.C., Smith B.F.L. & Wilson M.J. (editors) (1994) *Clay Mineralogy: Spectroscopy and Chemical Determinative Methods*. Chapman & Hall, New York, NY, USA.

Bennour A., Mahmoudi S., Srasra E., Hatira N., Boussen S., Ouaja M. & Zargouni F. (2015a) Identification and traditional ceramic application of clays from the Chouamekh region in south-eastern Tunisia. *Applied Clay Science*, **118**, 212–220.

Bennour A., Mahmoudi S., Srasra E., Boussen S. & Hatira N. (2015b) Composition, firing behavior and ceramic properties of the Sejnène clays (Northwest Tunisia). *Applied Clay Science*, **115**, 30–38.

Bowles J.E. (1992) *Engineering Properties of Soils and Their Measurement*. McGraw-Hill Inc., New York, NY, USA.

Brindley G.W. & Nakahira M. (1959) The kaolinite–mullite reaction series: II. Metakolin. *Journal of the American Ceramic Society*, **42**(7), 314–318.

Cengiz O. & Kuşçu M. (2010) Anamasdağları-Isparta terra rossalarının tuğla-kiremit üretiminde kullanılabilirliği. *Kibited*, **1**(4), 287–299.

Chang L.L.Y. (2002) *Industrial Mineralogy: Materials, Processes, and Uses*. Prentice Hall, Upper Saddle River, NJ, USA.

Chen P.Y. (1977) Table of key lines in X-ray powder diffraction patterns of minerals in clays and associated rocks. Geological Survey Occasional Paper 21, Indiana Geological Survey Report 21.

Çelik H. (2010) Technological characterization and industrial application of two Turkish clays for the ceramic industry. *Applied Clay Science*, **50**, 245–254.

https://doi.org/10.1180/clm.2018.40 Published online by Cambridge University Press

Dondi M., Ercolani G., Melandri C., Mingazzini C. & Marsigli M. (1999) The chemical composition of porcelain stoneware tiles and its influence on microstructural and mechanical properties. *Interceram*, **48**, 75–83.

Dondi M., Guarini G., Ligas P., Palomba M. & Raimondo M. (2001) Chemical, mineralogical and ceramic properties of kaolinitic materials from the Tresnuraghes mining district (Western Sardinia, Italy). *Applied Clay Science*, **18**, 145–155.

Dondi M., Guarini G., Raimondo M. & Salucci F. (2003) Influence of mineralogy and particle size on the technological properties of ball clays for porcelainized stoneware tiles. *Tile and Brick International*, **20**(2), 2–11.

Dondi M., Raimondo M. & Zanelli C. (2014) Clays and bodies for ceramic tiles: reappraisal and technological classification. *Applied Clay Science*, **96**, 91–109.

El Ouahabi M., Daoudi L. & Fagel N. (2014) Mineralogical and geotechnical characterization of clays from Northern Morocco for their potential use in ceramic industry. *Clay Minerals*, **49**, 1–17.

Fabbri B. & Fiori C. (1985) Clays and complementary raw materials for stoneware tiles. *Mineralogica Petrographica Acta*, **29A**, 535–545.

Grim R.E. & Rowland A.R. (2009) *Differential Thermal Analysis of Clay Minerals and Other Hydrous Materials, Part 1*. Mineralogical Society of America, Chantilly, VA, USA.

Grim R.E. (1962) *Applied Clay Mineralogy*. McGraw-Hill, NY, USA.

Holtz R.D. & Kovacs W.D. (1981) *An Introduction to Geotechnical Engineering*. Prentice Hall, Englewood Cliffs, NJ, USA.

Insley H. & Ewell R.H. (1935) Thermal behavior of kaolin minerals. *Journal of Research of the National Bureau of Standards, USA*, **14**, 615–627.

Jackson M.L. (1979) *Soil Chemical Analysis – Advanced Course*, 2nd edition. Published by the author, Madison, WI, USA.

Jones F.O. (1964) New fast accurate test measures bentonite in drilling mud. *Oil Gas Journal*, **42**, 76–78.

Konta J. (1995) Clay and man: clay raw materials in the service of man. *Applied Clay Science*, **10**, 275–335.

Kreimeyer R. (1987) Some notes on the firing color of clay bricks. *Applied Clay Science*, **2**, 175–183.

Lee V.G. & Yeh T.H. (2008) Sintering effects on the development of mechanical properties of fired clay ceramics. *Materials Science and Engineering*, **485**, 5–13.

Mahmoudi S., Srasra E. & Zargouni F. (2008) The use of Tunisian Barremian clay in the traditional ceramic industry: optimization of ceramic properties. *Applied Clay Science*, **42**, 125–129.

Mefire A., Njoya A., Fouateu R., Mache J.R., Tapon N.A., Nzeukou Nzeugang A., Melo Chinje U., Pilate P., Flament P., Siniapkine S., Ngono A. & Fagel N. (2016) Occurrences of kaolin in Koutaba (west Cameroon): mineralogical and physicochemical characterization for use in ceramic products. *Clay Minerals*, **50**, 593–606.

Milheiro F.A.C., Freire M.N., Silva A.G.P. & Holanda J. N.F. (2005) Densification behaviour of a red firing Brazilian kaolinitic clay. *Ceramics International*, **31**, 757–763.

Monteiro S.N. & Vieira C.M.F. (2004) Influence of firing temperature on the ceramic properties of clays from Campos dos Goytacazes, Brazil. *Applied Clay Science*, **27**, 229–234.

Moore D.M. & Reynolds J.R. (1989) *X-Ray Diffraction and the Identification and Analysis of Clay Minerals*. Oxford University Press, Oxford, UK.

Murray H.H. (2007) *Applied Clay Mineralogy. Developments in Clay Science*. Elsevier, Amsterdam, The Netherlands.

Ngun B.K., Mohamad H., Sulaiman S.K., Okada K. & Ahmad Z.A. (2011) Some ceramic properties of clays from central Cambodia. *Applied Clay Mineralogy*, **53**, 33–41.

Smoot T.W. (1961) Clay minerals in the ceramic industries. *Clays and Clay Minerals*, **10**, 309–317.

TCF (2009) Turkish Ceramics Federation, Ceramic Tile World Data.

Thorez J. (1976) *Practical Identification of Clay Minerals*. Lelotte, Dison, Belgium.

TS 4790 (1986) *Test Method for Common Bricks and Roofing Tile Clays*. Turkish Standards Institution, Ankara, Turkey.

TS EN 772-21 (2011) *Methods of Test for Masonry Units – Part 21: Determination of Water Absorption of Clay and Calcium Silicate Masonry Units by Cold Water Absorption*. Turkish Standards Institution, Ankara, Turkey.

TS EN 772-7 (2000) *Methods of Test for Masonry Units – Part 7: Determination of Water Absorption of Clay Masonry Damp Proof Course Units by Boiling in Water*. Turkish Standards Institution, Ankara, Turkey.

TS EN 771-1 (2012) *Specification for Masonry Units – Part 1: Clay Masonry Units*. Turkish Standards Institution, Ankara, Turkey.

Udvardi B., Kovács I.J., Kónya P., Földvári M., Füri J., Budai F., Falus G., Fancsik T., Szabó C., Szalai Z. & Mihály J. (2014) Application of attenuated total reflectance Fourier transform infrared spectroscopy in the mineralogical study of a landslide area, Hungary. *Sedimentary Geology*, **313**, 1–14.

Zaied F.H.B., Abidi R., Slim-Shimi N. & Somarin A.K. (2015) Potentiality of clay raw materials from Gram area (Northern Tunisia) in the ceramic industry. *Applied Clay Science*, **112–113**, 1–9.

Zanelli C., Iglesias C., Domínguez E., Gardini D., Raimondo M., Guarini G. & Dondi M. (2015) Mineralogical composition and particle size distribution as a key to understand the technological properties of Ukrainian ball clays. *Applied Clay Science*, **108**, 102–110.

https://doi.org/10.1180/clm.2018.40 Published online by Cambridge University Press